RSC Advances

PAPER

View Article Online
View Journal | View Issue

Cite this: *RSC Adv.*, 2017, **7**, 52907

Photocatalytic copper-catalyzed azide–alkyne cycloaddition click reaction with Cu(II) coordination polymer†

Xiangyang Guo, Le Zeng, Zhe Wang, Tiexin Zhang, Cheng He and Chunying Duan *

Received 14th September 2017
Accepted 30th October 2017

DOI: 10.1039/c7ra10207k

rsc.li/rsc-advances

A two dimensional Cu(II) coordination sheet has been developed. By incorporating well-designed chromophore linkers into the coordination polymer, the long conjugated system caused the maximum UV-vis absorption wavelength red shift to the visible area (up to 550 nm). Adjacent sheets were assembled in an ABAB fashion *via* π···π stacking and C–H···π interactions to form a three-dimensional structure. The interlayer stacking mode is important because its liability allows for exfoliation of the material which results in the dispersion of the active sites and the enhancement of the visible-light trapping capacity. Using this copper(II) coordination polymer, a series of click reactions were successfully conducted under household light irradiation in the air at room temperature. And 1,4-substituted triazoles were the single products in good yields. Moreover, the catalyst can be easily removed from the reaction mixture.

1. Introduction

The copper-catalyzed azide–alkyne cycloaddition (CuAAC) reaction is a hot research subject in click chemistry.[1–3] This reaction has been widely used in organic synthesis, medicinal chemistry, and polymer science.[4–7] Recently, this particularly powerful ligation reaction has been applied to biolabeling *in vivo*, due to its high degree of specificity and the biocompatibility of both starting materials. In previous work, a large variety of copper-related catalysts which provide Cu(I) species have been used for the important reaction. Such as the copper halide compounds, some improved Cu(I)-organic complexes, simple Cu(II) salts together with reducing agents and nano-structured solid catalysts.[8–15] However, the oxide species existing in the reaction system will influence the effect of Cu(I) catalysts and homogeneous catalytic systems are inconvenient with regards to the separation and purification of the product. As we all know, although copper is an essential element for humans, large and acute doses can have harmful, even fatal, effects.[16] In this case and due to the toxic properties of copper species *in vivo*, low loading of copper catalyst or mild reaction conditions, such as heterogeneous photocatalysis systems, should be applied.[17–19]

Coordination polymers are crystalline solids generated by the association of metal-containing secondary building units and multi-topic organic linkers through strong bonds.[20–22] Their function and application can be predicted through predesigned ligand and the selective active catalytic sites. Because of their unique attributes, low density, open structures with periodic dual compositions, and amenability to bottom-up assembly into a desired framework, these frameworks have emerged as very promising materials for heterogeneous catalysis, gas storage, drug delivery and photocatalysis over the past few decades.[23–30] So far, considerable work has been done on their application in catalytic field using functional linkers or active metal nodes of frameworks. And there have been only a few amusing researches about application of photocatalysis in organic synthesis using copper(II) coordination polymers.[31–34] Only a tiny amount of studies has been reported of using Cu(I) or the reduced Cu(II) coordination polymers as heterogeneous catalysts for 'click' reactions.[35–39] It is a challenge that use Cu(II) coordination polymers as photocatalyst for CuAAC reaction.

In this work, we report the synthesis of a two-dimensional (2D) Cu(II) coordination polymer Cu($C_{33}H_{19}NO_6S_3$) (denoted as Cu–**TCTA**); where H_3**TCTA** is 5,5′,5″-(nitrilotris(benzene-4,1-diyl))tris(thiophene-2-carboxylic acid); as the photocatalyst facilitates the important reaction (Scheme 1).[40] The introduction of the thiophene units into the triphenylamine which results in the increase of the conjugation. Compared with 4,4′,4″-tricarboxytriphenyl amine (H_3**TCA**, 390 nm), the maximum UV-vis absorption wavelength of H_3**TCTA** (450 nm) shifted toward long wavelength (Fig. S1a, ESI†). And the first oxidation potential is progressively shifted to more negative values with increasing size of the conjugated backbone.[41] By incorporate the well-designed chromophore linkers (H_3**TCTA**)

State Key Laboratory of Fine Chemicals, Dalian University of Technology, Dalian, 116024, P. R. China. E-mail: cyduan@dlut.edu.cn

† Electronic supplementary information (ESI) available: Characterization data, as well as additional tables and figures. CCDC 1536834. For ESI and crystallographic data in CIF or other electronic format see DOI: 10.1039/c7ra10207k

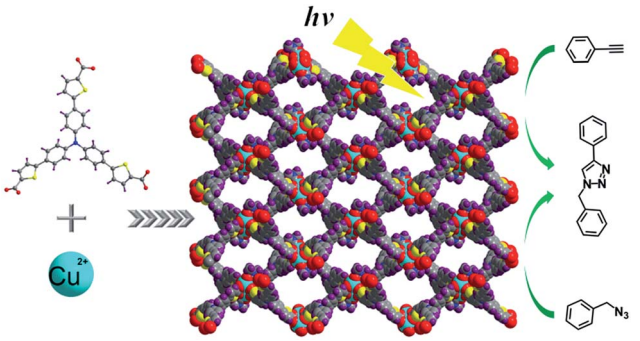

Scheme 1 Synthetic procedure of the Cu–**TCTA** and the design of CuAAC reaction under irradiation.

into the coordination polymer, Cu–**TCTA** exhibits a broad solid-state UV-vis absorption up to 550 nm (Fig. S1b, ESI†). It can be used to catalyse the click reaction under household light irradiation in air with co-catalyst. The catalytic activity was then demonstrated by a serious of cycloaddition reactions.

2. Results and discussion

2.1 Synthesis and characterization of Cu–TCTA

The two-dimension coordination polymer of Cu–**TCTA** (CCDC no. 1536834†) was synthesized through solvothermal reaction of $Cu(NO_3)_2 \cdot 3H_2O$ and H_3**TCTA** at 100 °C for 3 days produced oval-shaped crystals in the mixture of DMF and ethanol (v/v = 1 : 2), producing a yield of 57%. Elemental analyses and powder X-ray diffraction (XRD) analysis indicated the pure phase of its bulk sample. Single-crystal X-ray diffraction studies reveal that Cu–**TCTA** crystallizes in the monoclinic with space group $P2_1/c$. As shown in Fig. 1a, the asymmetric unit consists of one Cu(II) ion connected by one ligand and one coordinated DMF molecule. The copper atom is surrounded by four oxygen atoms from carboxyl groups of four different H_3**TCTA** ligands and one oxygen atom from DMF molecule to attain a five-coordinated square pyramidal geometry. The four carboxyl groups from four different ligands bridging Cu(1) and Cu(1A) (symmetry codes: A, $1-x, 2-y, -2-z$) forming the dinuclear paddle-wheel units. The Cu(II)–O distances and the bond angles of the adjacent donors around Cu(II) centre are in the range from 1.943(9)–2.158(9) Å and 87.9(4)–167.2(4)°, respectively. Each dinuclear paddle-wheel cluster is connected to four different deprotonated ligands to form two-dimensional layer structures. One of the three carboxyl groups of the ligands is uncoordinated (Fig. 1b). It is unlike the similar ligands.[42,43]

Since H_3**TCTA** has enormous flexibility as a supramolecular linker, it can be involved not only in coordination and hydrogen-bonds *via* its carboxyl groups, but also the uncoordinated arms of the ligands could form aromatic π···π stacking interactions.[44–46] As shown in Fig. 2a, the distance of the thiophene rings is 4.16 Å between the adjacent sheets. And the thiophene rings also have the C–H···π interactions with benzene rings of the another sheet. The distance and angle of C30–H30A···π is 3.39 Å and 143.7°, respectively. Adjacent sheets were assembled in an ABAB fashion *via* π···π stacking and C–H···π interactions to form a three-dimensional structure (Fig. 2b). When viewed along the *c* axis, each layer exhibits a large rhombic cages with a height of 17.27 Å and width of 34.48 Å (Fig. 1b). The packed structure exhibits 9.7 × 10.3 $Å^2$ one-dimension channels along the *c* axis after removed the coordinating DMF molecules (Fig. 1c). The interlayer stacking mode is important because of its liability allows for exfoliation of the material which results in the dispersion of the active sites and the enhancement of visible-light trapping capacity.[47,48] The effective free volume of Cu–**TCTA** was estimated to be 31.4% after removed the lattice solvent and the coordinating DMF by PLATON software.[49]

The introduction of the thiophene units results in the increase of the conjugation. As shown in Fig. 3a, the distances between the nitrogen-centred atom of **TCTA** fragment and the copper atoms of adjacent layers range from 7.72 to 11.05 Å, which is shorter than the coordinated copper atoms ranging from 11.35 to 12.33 Å. These shorter distances benefit Cu–**TCTA** forming the intermolecular charge transfer salts. Hence the copper nodes have certain properties of copper(I), leading to the framework presenting a weak fluorescence (Fig. 2b).[50,51]

Besides, the long π-conjugated system reduces the rate of back electron transfer and makes charge separation easy to control. And the first oxidation potential is progressively shifted to more negative values with increasing size of the conjugated backbone. Solid state cyclic voltammetry of Cu–**TCTA**

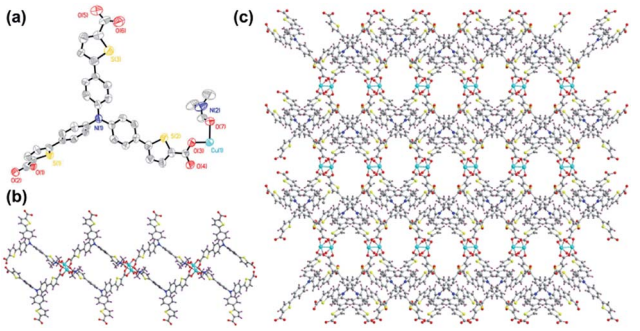

Fig. 1 (a) The ORTEP drawing of asymmetric unit of Cu–**TCTA**, the atoms are represented by 30% probability thermal ellipsoids; (b) perspective view of the 2D structure along the *b* axis and (c) along the *c* axis. Colour code: Cu, turquoise; S, yellow; N, blue; O, red; C, grey; H, violet. The lattice and coordinating solvents are omitted for clarity.

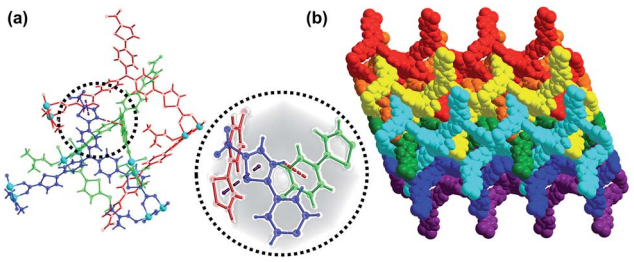

Fig. 2 (a) The interpenetration structure between 2D layers. (b) The 3D stacking structure of Cu–**TCTA** view along the *b* axis.

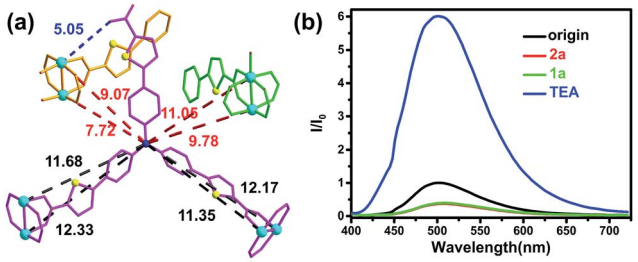

Fig. 3 (a) The distance of nitrogen centre of TCTA with copper cations in interpenetration structure. (b) Family of emission spectra of Cu–TCTA (0.05% in weight) in $CHCl_3$ suspension upon addition of **2a**, **1a** and TEA, excitation at 390 nm.

measurements exhibited (Fig. 4a) reversible redox band centred at 187 mV (*vs.* SCE) relative to the Cu^{II}/Cu^{I} redox couple and also an irreversible oxidative peak at 1.07 V (*vs.* SCE) relative to **TCTA**$^+$/**TCTA**. The transition energies (E^{0-0}) of H_3**TCTA** is 2.70 eV, which is lower than H_3**TCA** (E^{0-0} = 3.25 eV) (Fig. 4b). The redox potential of the excited-state H_3**TCTA**$^+$/H_3**TCTA*** couple was determined to be −1.63 V on the basis of transition energies.[52,53]

2.2 Photocatalytic properties of Cu–TCTA

To probe the catalytic activity of Cu–**TCTA** for the CuAAC, a series of experiments were performed to optimize the reaction conditions. Trimethylamine (TEA) was used as the electron donor (ED), instead of preventing copper(I) oxidation for most the azide–alkyne cycloaddition reaction. And the reaction of (azidomethyl) benzene (**1a**) and phenylacetylene (**2a**) was initially investigated with 28 W household light as light source at room temperature. Firstly, the reaction was tested with different solvents with 0.5 mol% photocatalytic loading (Table S2, ESI†). The reactions were monitored by means of ^{1}H NMR spectroscopy. And conversions were determined by integration of a particular signal from a proton in one of the starting molecules (4.3 ppm) and the corresponding proton in the product (5.5 ppm).[54] After standing the reaction mixture for several days, the colourless rod like crystal was obtained. The single crystal diffraction demonstrated that the product was 1,4-substituted triazole (**3a**) (Fig. S8, ESI†). There were relatively low yields in the solution of acetonitrile or ethanol under

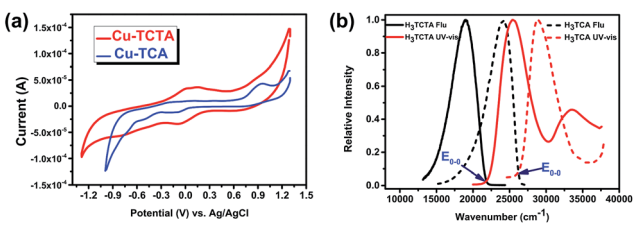

Fig. 4 (a) Solid state cyclic voltammetry of Cu–TCA (blue line) and Cu–TCTA (red line), scan rate: 100 mV s^{-1}. (b) Normalized absorption (red line) and emission spectrum (black line) of H_3TCA (dash line) and H_3TCTA (solid line) in DMF, excitation at 350 nm and 390 nm, respectively.

irradiation. Moderate catalytic activity was obtained for THF. When $CDCl_3$ was used as the solvent, the yield of **3a** was near 94% under irradiation and only 8.4% under dark after six hours. $CDCl_3$ was selected as the optimal solvent. Control experiments in the absence of TEA or in the presence of H_3**TCTA** were also performed, but just minimal amount of **3a** was detected under irradiation and no click reaction was detected under dark. In conclusion, the suitable reaction conditions: Cu–**TCTA** (0.5 mol%), azide/alkyne/amine (0.5 mmol : 0.5 mmol : 0.5 mmol), room temperature, 6 h, was chosen to study the catalytic activity.

In order to research the mechanism of photocatalytic CuAAC click reaction. The luminescence properties of Cu–**TCTA** was investigated when the substrates and co-catalyst were gradually added to the suspension of Cu–**TCTA** in $CHCl_3$. Cu–**TCTA** exhibited a weak luminescence band at 500 nm upon excitation at the wavelength of 390 nm. The luminescence was quenched upon addition of **2a**. Then the intensity of the emission at 500 nm was no significant change along the addition of **1a**. But the intensity was dramatically increase with TEA added into the mixture (Fig. 3b). By analogy with previous reports, a stepwise mechanism based on the observations for the photocatalytic reaction with Cu(II)-coordination polymers is proposed. It begins the Cu(II)-coordination polymers was reduced into Cu(I)-coordination polymers under irradiation, then the process as same as most azide–alkyne cycloaddition CuAAC reaction mechanism which was proposed by Fokin and co-workers from their DFT calculation.[2]

A detailed kinetic study of the reaction between **1a** and **2a** was conducted (Table S3, ESI†) to study the catalytic activity of Cu–**TCTA**. There was a very low conversion in the first hour. Two hours later, most of the substrates were converted into product, and almost quantitatively converted (yield, 94.3%) after six hours. When the catalytic reaction was stopped after 3 h, the supernatant was obtained by centrifugation and filtration. Just a 6.7% transformation was observed when subjected to standard conditions for another 3 h (Fig. S5, ESI†). These results clearly demonstrate that the azide–alkyne cycloaddition reaction majorly occurred in the heterogeneity fashion.[15,55,56]

After the reaction, Cu–**TCTA** was easily isolated from the reaction mixture by centrifugation. On the basis of the scanning electron microscopy and transmission electron microscopy images, the nanoscale thin layers were *in situ* exfoliated from the single-crystal blocks of 2D coordination polymers (Fig. 5a–c). The exfoliation was postulated to be due to the interlayer π⋯π stacking by the comprehensive effects of mechanical shearing forces during stirring, weak interactions relevant to the solvents and other compounds, and interlayer charge repulsions during the photoredox cycles. In addition, the indexing of the X-ray powder diffraction patterns of the recovered catalyst indicated that the integrity of the 2D coordination polymers was maintained during the reaction (Fig. 5d).[57]

Control experiment with Cu–**TCA** and MOF-150 was conducted under the same conditions. There was only 2% conversion for MOF-150 and trace amount of product for Cu–**TCA** (Fig. S7, ESI†). Dye uptake experiment (Fig. S2, ESI†) and IR spectrum (Fig. S3, ESI†) of Cu–**TCTA** soaked with azide and

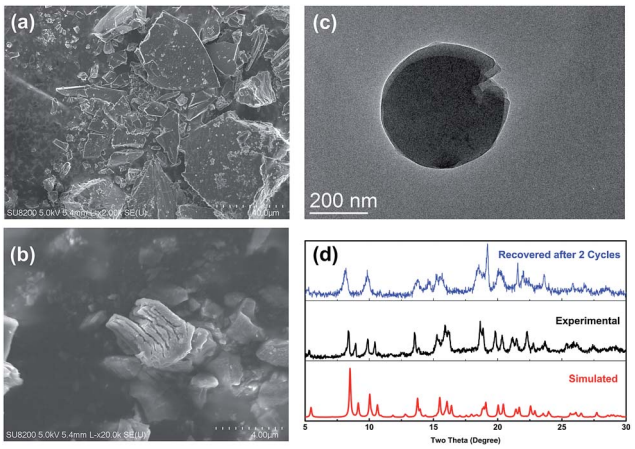

Fig. 5 (a) SEM image of Cu–**TCTA**; (b) SEM image of Cu–**TCTA** after catalysed; (c) TEM image of exfoliated thin layers and (d) simulated (red) and experimental (black) XRD patterns of the Cu–**TCTA** crystal and the experimental pattern of the catalyst recovered after 2 cycles of catalysis (blue).

alkyne revealed that the photocatalytic azide–alkyne cycloaddition reaction was the surface reaction on the catalyst. In order to demonstrated the surface catalytic reaction, the as-synthesized Cu–**TCTA** was used to conduct click reaction. The yield was only 7% at the same conditions (Fig. S7, ESI†). With the size of the microcrystals reduced to a few micrometres or nanometres by grinding Cu–**TCTA** crystals, the reaction of **1a** with **2a** has a dramatic increase conversion (>90%) than the as-synthesized catalyst, which size are hundred micrometres (Fig. S6, ESI†).

To evaluate the scope of this new Cu–**TCTA** catalysed process further, reaction of benzyl azide and 4-methylbenzyl azide with several aliphatic and aromatic terminal alkynes substituted by electron-donating/electron-withdrawing groups were conducted (Table 1). In all the cases, a single product 1,4-disubstituted 1,2,3-triazoles were obtained. And the substrates bearing electron-donating group such as methoxyl group (entries 3 and 8) or electron-withdrawing group such as cyan group (entries 5 and 10) at the *para* position of the phenyl ring are all suitable substrates.

Recyclability is an essential feature of any catalyst considered for use.[58] The reusability of the catalyst was tested for the reaction of **1a** and **2a** in $CDCl_3$ in air upon household light irradiation for 6 h. Though solid Cu–**TCTA** could be easily isolated from the reaction suspension by filtration, it could only be subsequently reused two times because of the unavoidable loss of small quantities of catalyst, with only slight decrease in its reactivity (yield, 90.2%). We also conducted the extensive experiment that using large excesses of **1a** (10 mmol), **2a** (10 mmol) and Cu–**TCTA** (2.5 μmol) while added 140 μL TEA every 12 hours. A small aliquot of the supernatant reaction mixture was analyzed by ^{1}H NMR to calculate the reaction yields. After 48 h reaction, the yield was 58.5%. It should be noted that such a considerable amount indicates that Cu–**TCTA** can be used into the laboratory practice.

Compared to previous works, our system does not require UV irradiation nor heating while still acquiring the same high product yields with similarly low catalyst loading. As it is

Table 1 Scope of the photocatalytic CuAAC[a]

Entry	Azide	Alkyne	Yield (%)
1	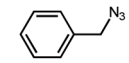	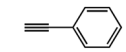	93.5
2	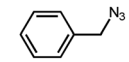	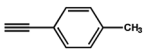	65.8
3	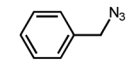	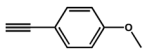	67.1
4	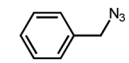	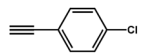	90.9
5	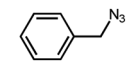	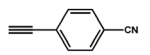	78.1
6	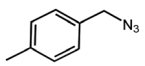	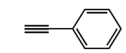	77.0
7	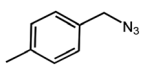	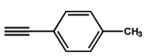	81.3
8	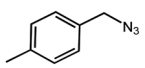	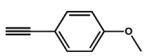	66.7
9	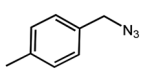	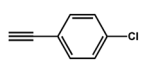	42.7
10	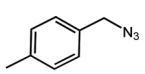	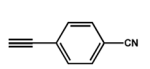	54.3

[a] Reaction conditions: Cu–**TCTA** (0.5 mol%), azide/alkyne/amine (0.5 mmol : 0.5 mmol : 0.5 mmol), room temperature, household light irradiation, 6 h. Yields were calculated by ^{1}H NMR analysis in $CDCl_3$.

a heterogeneously catalysed reaction it is easy to separate the catalyst from the mixture. However, there are still some problems such as poor recyclability and the currently unavoidable loss of catalyst.[35–38]

3. Experimental section

3.1 Reagents and instrumentation

All chemicals were of reagent-grade quality, obtained from commercial sources and used without further purification. The crystallographic data were collected on a Bruker SMART APEX CCD diffractometer with graphite-monochromated Mo-Kα radiation (λ = 0.71073 Å) using the SMART and SAINT programs. Elemental analyses of C, H and N were performed using a Vario EL III elemental analyzer. Fourier transform infrared spectroscopy (FT-IR) spectra were recorded using KBr pellets on a JASCO FT/IR-430. Powder X-ray diffraction (PXRD) measurements were obtained on a Rigaku SmartLab XRD instrument with a sealed Cu tube (λ = 1.54178 Å). Thermogravimetric analyses were performed on a Mettler-Toledo TGA/SDTA851 instrument and recorded under N_2 or air after 14 equilibrations at 100 °C followed by a ramp of 10 °C min^{-1} up to 800 °C. ^{1}H NMR was measured on a Varian INOVA-400 spectrometer with chemical shifts reported as ppm (in DMSO-

d_6 or $CDCl_3$, TMS as internal standard). The solid UV-vis spectra were recorded on a Hitachi U-4100 UV-VIS-NIR Spectrophotometer. Liquid UV-vis spectra were performed on a TU-1900 spectrophotometer. The fluorescent spectra were measured on Edinburgh FS920 Spectrometers. Transmission electron microscopy (TEM) images were collected on a Tecnai F30 operated at 300 kV. The excitation and emission slits were both 3 nm wide. Scanning electron microscopy (SEM) images were taken with a HITACHI UHR FE-SEM SU8200 microscope.

3.2 General methods

Solid-state voltammograms were measured by using a carbon-paste working electrode, and a well-ground mixture of each bulk sample and carbon paste (graphite and mineral oil) was set in the channel of a glass tube and connected to a copper wire. A platinum wire with a 0.5 mm diameter counter electrode and saturated calomel reference electrode were used. Measurements were performed by using a three electrode system in 0.1 M KNO_3 aqueous solution at a scan rate of 100 mV s^{-1}.

Dye-uptaking experiments were displayed by soaking **Cu–TCTA** (7.8 mg) in a CH_3CN solution of methylene blue dye (24 mM, 2 mL) overnight. The resulting crystalline powders were washed thoroughly with methanol until the solution became colorless. The washed samples were digested by concentrated hydrochloric acid in CH_3CN/methanol (v/v = 1 : 1), and the resultant clear solution with light olivine color was diluted to 10 mL. The concentration of methylene blue was determined by comparing the UV-vis absorption with a standard curve.

3.3 Synthetic procedures

Synthesis and characterization of ligand H_3TCTA. 3 mL Br_2 were added drop wisely to the solution of NaOH (7.20 g, 0.18 mol) in 30 mL water on ice bath, and further stirred for 20 min. The solution was transferred to a pressure-equalizing dropping funnel and was added dropwisely to a solution of 1,1′,1″-[nitrilotris(4,1-phenylenethiene-5,2-diyl)]triethanone (3.34 g, 5.4 mmol) in 50 mL 1,4-dioxane for 5 h at 45 °C. Then the mixture was put on ice-bath, a saturated aqueous solution of hydroxylamine-HCl was added to quench the excessive sodium hypobromite. Then the mixture was acidified to about pH 3 with 1 mmol mL^{-1} HCl solution, the precipitate was filtered and dried under vacuum. The crude product was recrystallized from acetic acid to afford pure product as a yellowish solid (2.42 g, 72%). ^{1}H NMR (400 MHz, DMSO-d_6) δ = 13.10 (br s, 3H, acid), 7.75–7.69 (m, 9H, Ph and thiophene), 7.51 (d, J = 3.9 Hz, 3H, thiophene), 7.15 (d, J = 8.7 Hz, 6H, Ph); ^{13}C NMR (126 MHz, DMSO-d_6) δ = 162.8, 149.4, 146.7, 134.4, 132.6, 128.0, 127.3, 124.4, 123.9. FTIR (KBr pellet; cm^{-1}): 3456, 2852, 1674, 1596, 1536, 1508, 1448, 1322, 1276, 1186, 1103, 1037, 812, 747 cm^{-1}. HRMS (ESI) m/z calcd for $C_{33}H_{20}NO_6S_3$ [M^+] 622.0453, found 622.0467.

Synthesis of Cu–TCTA. H_3**TCTA** (20 mg, 0.032 mmol) and $Cu(NO_3)_2 \cdot 3H_2O$ (36 mg, 0.15 mmol) were dissolved in 6 mL of mixed solvent containing dimethylformamide (DMF) and ethanol in a screw-capped vial. The resulting mixture was kept in an oven at 110 °C for 2 days. After cooling the oven to room temperature, yellow-green, block-shaped single crystals were separated, washed with ethanol and dried naturally at room temperature. The reaction yield based on the weight of the solvent-free material was approximately 52% relative to H_3**TCTA**. Anal. calcd for $CuC_{39}H_{35}N_3O_8S_3$: C 56.33, H 4.00, N 5.05%. Found: C 53.05, H 4.38, N 6.32%. IR (KBr): 3027 (w), 1659 (s), 1597 (s), 1536 (s), 1505 (m), 1449 (vs), 1395 (vs), 1273 (s), 1184 (m), 1101 (m), 812 (m), 768 (w), 667 (w) cm^{-1}.

3.4 Catalysis details

Typical procedure for the photocatalytic CuAAC reaction. Cu–**TCTA** (0.5 mol%) was dispersed in 1.5 mL of $CDCl_3$ in a quartz test tube and then the correspondent amount of each reactant (azide/alkyne/amine (0.5 mmol : 0.5 mmol : 0.5 mmol)) was added. The reaction mixture was stirred and irradiated with household light at room temperature and under air for 6 h. The solid catalyst was separated by filtration. The reactions were monitored by means of ^{1}H NMR spectroscopy. And conversions were determined by integration of a particular signal from a proton in one of the starting molecules (4.3 ppm) and the corresponding proton in the product (5.5 ppm).

Synthesis the substrates 1a and 1b. The benzyl azides were synthesized by the following protocol:[11] the proper benzyl halide (benzyl chloride or 4-methylbenzyl bromide) was dissolved (50 mmol, 1 equiv.) in 120 mL of dimethyl sulfoxide (DMSO) in a one-necked flask. Sodium azide (75.8 mmol, 1.45 equiv.) was then added to the reaction flask and the reaction mixture was stirred at room temperature overnight. The resulting product was extracted by ethyl acetate. The organic phase was washed with saturated NaCl solution and dried over Na_2SO_4. Finally, the solvent was removed under vacuum leading to pale yellow oil. The products were characterized by ^{1}H NMR. Benzyl azide: ^{1}H NMR (400 MHz, $CDCl_3$) δ: 7.29–7.38 (m, 5H), 4.30 (s, 2H). 4-Methylbenzyl azide: ^{1}H NMR (300 MHz, $CDCl_3$) δ: 7.11 (s, 4H), 4.19 (s, 2H), 2.27 (s, 3H).

4. Conclusions

In a summary, a new 2D copper(II) coordination polymer has been prepared using elaborately designed ligand of thiophenyl triphenylamine carboxylic acid derivatives. The long conjugated system caused the maximum UV-vis absorption wavelength red shift to the visible area and reduced the recombination velocity of electrons and holes. Using this copper(II) coordination polymer, a series of click reactions were successfully conducted under the household light irradiation in air with the presence of trimethylamine. The 1,4-substituted triazoles were the single products and have good yields. And it features high catalytic activity, rapid dynamics of the substrate to product transformation. Moreover, the catalyst can be easily removed from the reaction mixture.

Conflicts of interest

There are no conflicts to declare.

Acknowledgements

We gratefully acknowledge the financial support from the National Natural Science Foundation of China (21531001, 21402020 and U1608224).

Notes and references

1 H. C. Kolb, M. G. Finn and K. B. Sharpless, *Angew. Chem., Int. Ed.*, 2001, **40**, 2004–2021.
2 F. Himo, T. Lovell, R. Hilgraf, V. V. Rostovtsev, L. Noodleman, K. B. Sharpless and V. V. Fokin, *J. Am. Chem. Soc.*, 2005, **127**, 210–216.
3 J. E. Moses and A. D. Moorhouse, *Chem. Soc. Rev.*, 2007, **36**, 1249–1262.
4 O. Altintas and U. Tunca, *Chem.–Asian J.*, 2011, **6**, 2584–2591.
5 O. Altintas, U. Tunca and C. Barner-Kowollik, *Polym. Chem.*, 2011, **2**, 1146–1155.
6 O. Altintas, A. P. Vogt, C. Barner-Kowollik and U. Tunca, *Polym. Chem.*, 2012, **3**, 34–45.
7 A. J. Teator, D. N. Lastovickova and C. W. Bielawski, *Chem. Rev.*, 2016, **116**, 1969–1992.
8 L. Y. Liang and D. Astruc, *Coord. Chem. Rev.*, 2011, **255**, 2933–2945.
9 C. L. Wang, D. Ikhlef, S. Kahlal, J.-Y. Saillard and D. Astruc, *Coord. Chem. Rev.*, 2016, **316**, 1–30.
10 L. Ackermann, H. K. Potukuchi, D. Landsberg and R. Vicente, *Org. Lett.*, 2008, **10**, 3081–3084.
11 A. L. Schöffler, A. Makarem, F. Rominger and B. F. Straub, *Beilstein J. Org. Chem.*, 2016, **12**, 1566–1572.
12 S. J. Gu, J. H. Du, J. J. Huang, H. Xia, L. Yang and W. L. Xu, *Beilstein J. Org. Chem.*, 2016, **12**, 863–873.
13 K. Namitharan, M. Kumarraja and K. Pitchumani, *Chem.–Eur. J.*, 2009, **15**, 2755–2758.
14 K. Yamaguchi, T. Oishi, T. Katayama and N. Mizuno, *Chem.–Eur. J.*, 2009, **15**, 10464–10472.
15 B. W. Wang, J. Durantini, J. Nie, A. E. Lanterna and J. C. Scaiano, *J. Am. Chem. Soc.*, 2016, **138**, 13127–13130.
16 Y. Bai, X. Feng, H. Xing, Y. Xu, B. K. Kim, N. Baig, T. Zhou, A. A. Gewirth, Y. Lu, E. Oldfield and S. C. Zimmerman, *J. Am. Chem. Soc.*, 2016, **138**, 11077–11080.
17 E. Bigagli, C. Luceri, S. Bernardini, A. Dei and P. Dolara, *Chem.-Biol. Interact.*, 2010, **188**, 214–219.
18 C. Testa, M. Scrima, M. Grimaldi, A. M. D'Ursi, M. L. Dirain, N. L. Germain, A. Singh, C. H. Luevano, M. Chorev, P. Rovero and A. M. Papini, *J. Med. Chem.*, 2014, **57**, 9424–9434.
19 V. Bevilacqua, M. King, M. Chaumontet, M. Nothisen, S. Gabillet, D. Buisson, C. Puente, A. Wagner and F. Taran, *Angew. Chem., Int. Ed.*, 2014, **53**, 5872–5876.
20 H. Li, M. Eddaoudi, M. O'Keeffe and O. M. Yaghi, *Nature*, 1999, **402**, 276–279.
21 S. R. Batten, N. R. Champness, X. M. Chen, J. Garcia-artinez, S. Kitagawa, L. Öhrström, M. O'Keeffe, M. Paik Suh and J. Reedijk, *Pure Appl. Chem.*, 2013, **85**, 1715–1724.
22 H. Zhou, J. R. Long and O. M. Yaghi, *Chem. Rev.*, 2012, **112**, 673–674.
23 J. Liu, L. Chen, H. Cui, J. Zhang, L. Zhang and C. Y. Su, *Chem. Soc. Rev.*, 2014, **43**, 6011–6061.
24 A. Corma, H. García and F. X. Llabrés i Xamena, *Chem. Rev.*, 2010, **110**, 4606–4655.
25 C. Wang, Z. G. Xie, K. E. de Kafft and W. B. Lin, *J. Am. Chem. Soc.*, 2011, **133**, 13445–13454.
26 M. H. Alkordi, Y. Liu, R. W. Larsen, J. F. Eubank and M. Eddaoudi, *J. Am. Chem. Soc.*, 2008, **130**, 12639–12641.
27 J. Lee, O. K. Farha, J. Roberts, K. A. Scheidt, S. T. Nguyen and J. T. Hupp, *Chem. Soc. Rev.*, 2009, **38**, 1450–1459.
28 H. Furukawa, N. Ko, Y. B. Go, N. Aratani, S. B. Choi, E. Choi, A. O. Yazaydin, R. Q. Snurr, M. O'Keeffe, J. Kim and O. M. Yaghi, *Science*, 2010, **329**, 424–428.
29 M. Yoon, R. Srirambalaji and K. Kim, *Chem. Rev.*, 2012, **112**, 1196–1231.
30 C. Wang, D. Liu and W. B. Lin, *J. Am. Chem. Soc.*, 2013, **135**, 13222–13234.
31 B. J. Adzima, Y. H. Tao, C. J. Kloxin, C. A. DeForest, K. S. Anseth and C. N. Bowman, *Nat. Chem.*, 2011, **3**, 256–259.
32 M. A. Tasdelen and Y. Yagci, *Angew. Chem., Int. Ed.*, 2013, **52**, 5930–5938.
33 X. L. Wang, J. Luan, F. F. Sui, H. Y. Lin, G. C. Liu and C. Xu, *Cryst. Growth Des.*, 2013, **13**, 3561–3576.
34 J. F. Wang, C. Li, Q. X. Zhou, W. B. Wang, Y. J. Hou, B. W. Zhang and X. S. Wang, *Dalton Trans.*, 2016, **45**, 5439–5443.
35 Q. Fu, K. Xie, S. Tan, J. M. Ren, Q. Zhao, P. A. Webley and G. G. Qiao, *Chem. Commun.*, 2016, **52**, 12226–12229.
36 Z. H. Xu, L. L. Han, G. L. Zhuang, J. Bai and D. Sun, *Inorg. Chem.*, 2015, **54**, 4737–4743.
37 I. Luz, F. X. Llabrés i Xamena and A. Corma, *J. Catal.*, 2010, **276**, 134–140.
38 P. Li, S. Regati, H. C. Huang, H. D. Arman, J. C.-G. Zhao and B. L. Chen, *Inorg. Chem. Front.*, 2015, **2**, 42–46.
39 M. A. Tasdelen, B. Kiskan and Y. Yagci, *Prog. Polym. Sci.*, 2016, **52**, 19–78.
40 Data for Cu–TCTA: $C_{39}H_{32}CuN_3O_8S_3$, Mr = 830.39, monoclinic, space group $P2(1)/c$, a = 16.213(13) Å, b = 19.359(14) Å, c = 12.323(9) Å, β = 90.991(12)°, V = 3867(5) Å^3, Z = 4, of 6803 reflections, 1553 unique (R_{int} = 0.1454). Final R_1 [with $I > 2\sigma(I)$] = 0.0802, wR_2 (all data) = 0.2434 and S = 0.985. CCDC no. 1536834.
41 K. Idzik, J. Sołoducho, M. Łapkowski and S. Golba, *Electrochim. Acta*, 2008, **53**, 5665–5669.
42 P. Y. Wu, J. Wang, Y. M. Li, C. He, Z. Xie and C. Y. Duan, *Adv. Funct. Mater.*, 2011, **21**, 2788–2794.
43 P. Y. Wu, J. Wang, C. He, X. L. Zhang, Y. T. Wang, T. Liu and C. Y. Duan, *Adv. Funct. Mater.*, 2012, **22**, 1698–1703.
44 C. Livage, N. Guillou, A. Castiglione, J. Marrot, M. Frigoli and F. Millange, *Microporous Mesoporous Mater.*, 2012, **157**, 37–41.
45 H. K. Chae, J. Kim, O. D. Friedrichs, M. O'Keeffe and O. M. Yaghi, *Angew. Chem., Int. Ed.*, 2003, **42**, 3907–3909.
46 E. Y. Lee, S. Y. Jang and M. P. Suh, *J. Am. Chem. Soc.*, 2005, **127**, 6374–6381.

47 F. J. M. Hoeben, P. Jonkheijm, E. W. Meijer and A. P. H. J. Schenning, *Chem. Rev.*, 2005, **105**, 1491–1546.
48 A. C. Grimsdale and K. Müllen, *Angew. Chem., Int. Ed.*, 2005, **44**, 5592–5629.
49 A. L. Spek, *PLATON: A Multipurpose Crystallographic Tool*, Utrecht University, Utrecht, The Netherlands, 2001.
50 B. D. McCarthy, E. R. Hontz, S. R. Yost, T. V. Voorhis and M. Dinca, *J. Phys. Chem. Lett.*, 2013, **4**, 453–458.
51 T. P. Liu, L. H. Huo, Z. P. Deng, H. Zhao and S. Gao, *RSC Adv.*, 2014, **4**, 40693–40710.
52 G. J. Kavarnos, *Fundamentals of Photoinduced Electron Transfer*, VCH, New York, 1993.
53 D. Rehm and A. Weller, *Isr. J. Chem.*, 1970, **8**, 259–271.
54 M. A. Tasdelen and Y. Yagci, *Tetrahedron Lett.*, 2010, **51**, 6945–6947.
55 J. S. Wang, F. Z. Jin, H. C. Ma, X. B. Li, M. Y. Liu, J. L. Kan, G. J. Chen and Y.-B. Dong, *Inorg. Chem.*, 2016, **55**, 6685–6691.
56 A. Chakraborty, S. Bhattacharyya, A. Hazra, A. C. Ghosh and T. K. Maji, *Chem. Commun.*, 2016, **52**, 2831–2834.
57 M. Zhao, Q. Lu, Q. Ma and H. Zhang, *Small Methods*, 2017, **1**, 1600030.
58 Z. Zhou, L. Yang, Y. F. Wang, C. He, T. Liu and C. Y. Duan, *RSC Adv.*, 2016, **6**, 108010–108016.